LAWRENCE
LIVERMORE
NATIONAL
LABORATORY

LLNL-JRNL-765557

Ocean barrier layers in the Energy Exascale Earth System Model

J. E. Jack Reeves Eyre, L. Van Roekel, X. Zheng, M. A. Brunke, J. C. Golaz

January 11, 2019

Geophysical Research Letters

Disclaimer

Ocean barrier layers in the Energy Exascale Earth System Model

J. E. Jack Reeves Eyre[1], Luke Van Roekel[2], Xubin Zeng[1], Michael A. Brunke[1]and Jean-Christophe Golaz[3]

[1]Department of Hydrology and Atmospheric Sciences, University of Arizona, Tucson, Arizona
[2]T-3, Fluid Dynamics and Solid Mechanics, Los Alamos National Laboratory, Los Alamos, New Mexico
[3]Lawrence Livermore National Laboratory, Livermore, California

Key Points:

- E3SMv1 simulates barrier layers in the correct locations and seasons, but with some thickness errors.
- In E3SMv1, barrier layers inhibit mixed layer entrainment of cold deep water in the tropics, but not in high latitudes.
- Atmosphere model biases affect barrier layer simulation fidelity, mainly through precipitation and evaporation in the tropics.

Corresponding author: Jack Reeves Eyre, jeyre@email.arizona.edu

Abstract

Ocean barrier layers (BLs) separate the mixed layer from the top of the thermocline, and are able to insulate the mixed layer from entrainment of cold thermocline water. Here, we provide the first global BL assessment in E3SMv1 and two other earth system models. Compared to observations, models reproduce the global distributions as semi-permanent features in some tropical regions and seasonal features elsewhere. However, model BLs are generally too thin in tropical regions and too thick in higher latitudes. BLs' ability to insulate the ocean surface from entrainment of cold thermocline water is most apparent in the tropics. Thus, E3SMv1s BL thickness (BLT) biases most affect entrainment here. Tropical BLT biases appear driven by atmosphere biases, mainly through the effect of precipitation minus evaporation (P-E) on mixed layer depth (MLD). At higher latitudes BLT biases are dominated by thermocline depth errors related to ocean circulation and vertical mixing.

1 Introduction

Barrier layers (BLs) were first analyzed around 30 years ago, using observations from the tropical West Pacific (Godfrey & Lindstrom, 1989; Lukas & Lindstrom, 1991). These initial studies showed that the ocean mixed layer (defined by near-constant density) can be vertically separated from the top of the thermocline by a near-isothermal but salt-stratified layer — the BL. In addition, it was recognized (Anderson et al., 1996; Lukas & Lindstrom, 1991) that BLs could insulate the upper ocean from entrainment of relatively cold, deep ocean water. Since these initial studies, BLs have been studied in other tropical oceans (e.g., Sprintall & Tomczak, 1992) and higher latitudes (e.g., Kara et al., 2000; Pan et al., 2018; Sato et al., 2006), and a diverse range of formation mechanisms have been identified (de Boyer Montégut et al., 2007; Mignot et al., 2007).

The role of the BL insulation effect in tropical ocean-atmosphere interactions has received much attention (e.g., Balaguru, Chang, Saravanan, & Jang, 2012; Drushka et al., 2014; Foltz & McPhaden, 2009; Maes et al., 2005). Away from the tropics the possible BL insulation effect has not been widely discussed in the literature, though associated salinity stratification has been shown to affect sea ice evolution (e.g., Duffy & Caldeira, 1997; Nguyen et al., 2009; Steele & Boyd, 1998). Because extratropical [JRE]mixed layers can be deeper, and BLs thicker, ~~in the extratropics, how much (if at all)~~[JRE]the strength of[JRE] the insulation effect remains~~occurs is~~[JRE] an open question.

Earth system models (ESMs) have been used to investigate BL formation (e.g., Balaguru, Chang, Saravanan, Leung, et al., 2012; Mignot et al., 2012) and BL effects on global and regional climate (e.g., Maes et al., 2002, 2005; Vialard & Delecluse, 1998; Zhu et al., 2014). Some of these studies have included brief validation of model BL characteristics, while more in-depth regional assessments of model BLs were performed by Zhi et al. (2016) in the West Pacific, and Breugem et al. (2008) and Balaguru, Chang, Saravanan, Leung, et al. (2012) in the tropical Atlantic. However, a global picture of model BLs is lacking and here we present what is, to our knowledge, the first ESM assessment of global BLs.

We also examine possible causes of model BL biases. [JRE]Since tropical BLs were first observed, freshwater input due to intense convective rainfall has been recognized as an important BL forcing (e.g., Lukas & Lindstrom, 1991; Sprintall & Tomczak, 1992; You, 1998). Thus, model biases in precipitation may contribute to BL biases, at least regionally. However, the size of this potential contribution is unclear, because precipitation usually acts in tandem with other forcings (Bosc et al., 2009; Mignot et al., 2007), including ocean advective processes (e.g., Cronin & McPhaden, 2002) and freshwater input from river runoff (Foltz et al., 2004; Pailler et al., 1999; Shenoi et al., 2002). Furthermore, there are regions where BL formation is almost entirely due to ocean circulation, such as the Southern Ocean (Pan et al., 2018), subtropical gyres (Sato et al., 2006) and the southeastern Arabian Sea (de Boyer Montégut et al., 2014).

Our assessment aims to answer three questions: (1) How well are BLs simulated in three leading Earth System Models? (2) What effect do BL thickness (BLT) biases have on upper ocean heat budgets? (3) Are model BLT biases caused by deficiencies in the ocean model, the atmosphere model, or coupled model interactions?

2 Data and methods

2.1 Model output

The ESM we focus on here is the recently released Energy Exascale Earth System Model version 1 (E3SMv1; E3SM Project, 2018). E3SMv1 is being developed by the U.S. Department of Energy to simulate and predict long-term changes in the climate system, with the goal of informing energy sector decision making. It is descended from the Community Earth System Model version 1 (CESM; Hurrell et al., 2013), but has diverged in several components, including some that have never before been used in a fully cou-

pled ESM. Notably E3SMv1 uses the Model for Prediction Across Scales Ocean model (MPAS-O; Petersen et al., 2019). Further details of E3SMv1 and the pre-industrial control run used here are given in Golaz et al. (2019) and references therein. Our investigations during the development of E3SMv1 exposed biases in western equatorial Pacific salinity stratification, and the present work has grown from these investigations.

We use monthly output from two E3SMv1 model runs: the E3SMv1 coupled pre-industrial control run (denoted here as E3SM-C); an E3SMv1 ocean-sea ice run (denoted here as E3SM-O) forced with COREv2 atmospheric reanalysis data (Large & Yeager, 2009) which includes surface salinity restoring. We also include the Community Earth System Model version 2.0.0 (CESM2; National Center for Atmospheric Research (NCAR), 2018) coupled pre-industrial control run; and the Geophysical Fluid Dynamics Laboratory (GFDL) Ensemble Coupled Data Assimilation version 3.1 (GFDL-ECDA-v3.1; Chang et al., 2013; Geophysical Fluid Dynamics Laboratory, 2013). The motivations for comparing E3SM-C to these particular models are: CESM2 is the same type of simulation (coupled pre-industrial control) using a similar class of model; GFDL-ECDA-v3.1 may be seen as a limit of how accurate a coupled ESM can be when constrained by historical observations (despite remaining MLD biases pertinent to BL simulation (Chang et al., 2013)); and E3SM-O sheds light on the behavior of MPAS-O without the confounding influence of biases from other components and from coupling.

We assess these four model runs using the same observational climatologies even though the comparison is not entirely fair. The difference in phasing of internal climate variability is a potential source of apparent bias in (fully coupled) E3SM-C and CESM2 that is not present in GFDL-ECDA-v3.1 and E3SM-O. However, analysis of E3SM-C suggests that differences (as a fraction of mean value) in BLT climatology from non-overlapping 30-year periods are small, so internal variability is not expected to be a major contributor to mean biases.

Further details on the model data are given in Supplementary Information, but we note here that the grid spacing of ocean models in all four model runs is comparable: of order 1° x 1° in the horizontal and 10 m in the vertical for the first 15-20 model levels, increasing with depth. Potential temperature, salinity and (where available) potential density are used from all four model runs. Conversion between oceanographic quantities is performed using the Gibbs Seawater Oceanographic Toolbox of the Thermody-

namic Equation of State 2010 (TEOS-10; McDougall & Barker, 2011; TEOS-10 Project, 2017). Precipitation, evaporation and the wind stress magnitude are used from E3SM-C, CESM2 and GFDL-ECDA-v3.1. Long-term averages used in most of our analysis are based on 60-year means for E3SM-C, E3SM-O and CESM2. For GFDL-ECDA-v3.1, we found that tropical Pacific BLs had a discontinuity around 1980, possibly related to changes in the number and type of assimilated observations, so we use 1981-2010 means.

2.2 Calculation of barrier layer thickness

BLT~~The barrier layer thickness (BLT)~~[JRE] is calculated, as in de Boyer Montégut et al. (2007), from the top of thermocline depth (TTD) and the mixed layer depth (MLD) using $BLT = TTD - MLD$. TTD is calculated as the depth where potential temperature first falls below $\theta_1 - \Delta\theta$, where θ_1 is the potential temperature of the top model layer and $\Delta\theta = 0.2$ °C (consistent with de Boyer Montégut et al. (2007)). MLD is calculated as the depth where potential density first exceeds $\sigma_1 + \Delta\sigma$. Here, $\Delta\sigma$ is a variable density threshold corresponding to the fixed temperature threshold used in TTD: $\Delta\sigma = \sigma(\theta_1 - 0.2, S_1) - \sigma(\theta_1, S_1)$, where S_1 is the absolute salinity of the top model layer. θ and σ are linearly interpolated between mid-depths of model levels (see schematic in Figure S1). In contrast with the method of de Boyer Montégut et al. (2007), to ensure consistency between different models, here we calculate BLT from monthly mean temperature, salinity and density fields, rather than calculating BLT at each time step and then averaging. Comparison between the two methods for isothermal layer depth (ILD; the depth where potential temperature first falls outside of $\theta_1 \pm \Delta\theta$), the only comparable variable in the E3SM-C output,~~from E3SM-C~~[JRE] results in mean absolute error of ~ 4 m. Basing this error quantification on ILD instead of MLD may slightly underestimate the error (as MLD can vary more in time than ILD) but the order of magnitude is probably correct.

2.3 Gridded observations

Model BLT, MLD and TTD are compared with the IFREMER observation-based climatology (de Boyer Montégut et al., 2007; Mignot et al., 2009; de Boyer Montégut et al., 2009). This climatology is based on ocean profiles from a range of instrument types (de Boyer Montégut et al., 2007) over the period 1961 to 2008. IFREMER includes several years of Argo data, but the number of Argo profiles has greatly increased (and their

vertical resolution has improved) since this dataset was created~~constructed~~[JRE]. The newer Scripps[JRE] MLD climatology ~~of~~ [JRE](Holte et al., 2017) is based on Argo data from 2000 to 2018 and so is potentially more representative~~complete and accurate~~[JRE]. However, it does not include the TTD quantity as calculated in de Boyer Montégut et al. (2007), and instead provides ILD: using this (instead of TTD) to calculate BLT results in significant differences where ocean temperature inversions occur (mostly midlatitudes, but also some tropical regions (de Boyer Montégut et al., 2007)). Nonetheless, the comparison of these two observational climatologies is a useful check: the two agree closely in tropical regions (mean BLT [JRE]difference = 0.3 m; see Table S1 and Figure S2), suggesting that the inclusion of more Argo data does not significantly affect BLT here. The midlatitude BLT~~mean~~[JRE] difference is larger ~~in midlatitudes~~ [JRE](Figure S2). The relatively good agreement in midlatitude MLD from the two datasets (Figure S3) suggests that BLT differences here are~~,~~[JRE] likely due to the inversion issue mentioned previously.

Model precipitation and evaporation are combined to give (P-E), which is compared with an estimate of mean 1981-2010 (P-E) from GPCP precipitation (which combines microwave and infrared satellite data with rain gauge observations; Adler et al., 2003, 2017) and OAFlux evaporation (which applies a bulk flux algorithm to near-surface variables from satellite and reanalysis data; Yu & Weller, 2007; Yu et al., 2006). Model wind stress is compared with the 1977-2006 mean from COREv2 (which is based on satellite-adjusted reanalysis data; Large & Yeager, 2009; Yeager & Large, 2008). Further details of the observational datasets are given in the Supplementary Information. To allow comparison of different datasets and variables, all observations and model output (with the exception of E3SM entrainment estimates) are bilinearly interpolated to the 2° x 2° IFREMER grid. Throughout our results, the term bias indicates model minus observations and the term difference indicates model minus model. Comparisons are limited to the region between 60°S and 60°N, and further masked to exclude regions where E3SM-C sea ice extends into this latitude range.

2.4 E3SM Entrainment cooling

For E3SM-C and E3SM-O, ocean model potential temperature tendencies were saved as part of the model output. This includes tendencies due to horizontal and vertical advection, surface heat fluxes, transmission of short-wave radiation below the surface, and separate local and non-local vertical turbulent mixing terms. We use the monthly mean

temperature tendency due to local vertical mixing, taking a depth-weighted average over all model levels in the mixed layer, to calculate entrainment cooling of this layer. The non-local vertical mixing is found to be small over the majority of the oceans and is thus ignored in this analysis. This part of the analysis, including comparison with model BLT, is performed on the native MPAS-O grid.

3 Results

3.1 Model-simulated mean BLT

The main features of the annual mean BLT (Figure 1a) from the IFREMER climatology are thick~~deep~~[JRE] barrier layers in midlatitudes (30°-60°, both hemispheres) and thinner~~shallower~~[JRE] barrier layers in the tropics (30°S-30°N). Note that the negative values in the north-east Atlantic and the northern periphery of the Southern Ocean are referred to as compensated layers (de Boyer Montégut et al., 2004); as this is not a focus of this work, we do not address these further. The ESMs generally have positive BLT biases (barrier layers too thick) in the midlatitudes and negative biases (barrier layers too thin) in the tropics (Figure 1). On average, midlatitude biases are of larger magnitude than tropical biases. In the case of E3SM-C (and, to a lesser extent, E3SM-O) midlatitude BLs extend too far equatorward. Notable exceptions to the general pattern are the positive biases around the maritime continent in all three coupled model runs, and negative biases in some parts of the Southern Ocean in CESM2.

To quantify biases, we consider grid points with observed annual mean BLT greater than 5 m. Such a thin BL could not be robustly portrayed by the models in this study, which have upper ocean vertical resolution ∼10 m, but this threshold is used to capture BLs that occur intermittently due to seasonal and interannual variability. The mean bias between 30°S and 30°N is -3.1 m for the E3SM-C (Table S1; the other model runs vary from -2.0 to -3.6 m). Midlatitude biases are much larger (e.g., +257 m for E3SM-C between 30°S and 60°S; see Table S1) and indicate that model BLs can be more than twice as thick as observed. Figure 1 shows that the region south of 50°S has particularly large biases in all model runs. Notable exceptions to the general pattern are the positive biases around the maritime continent in all three coupled model runs, and negative biases in some parts of the Southern Ocean in CESM2. In most regions, GFDL-ECDA-v3.1 has the smallest mean bias and mean absolute error (Figure 1; Table S1), suggesting that

the data assimilation is having a positive impact on the representation of JRE near- JRE surface temperature, salinity and density ~~profiles~~ JRE.

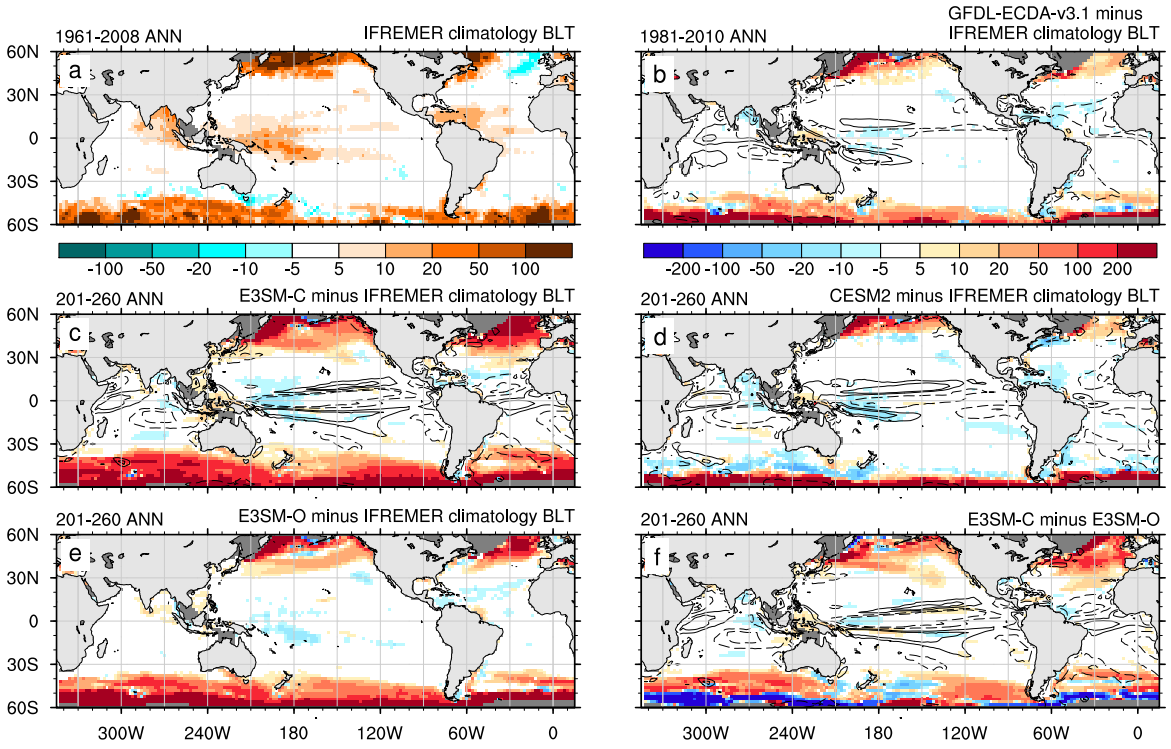

Figure 1. (a) Annual mean barrier layer thickness from IFREMER climatology, and biases relative to this of (b) GFDL-ECDA-v3.1, (c) E3SM-C, (d) CESM2 and (e) E3SM-O; (f) difference between annual mean BLT in E3SM-C and E3SM-O (equivalently, panel (c) minus (e)). In panels (b), (c), (d) and (f), contour lines show the bias of (precipitation minus evaporation) with solid contours at +1.0 and +2.0 mm day^{-1}, and dashed contours at -1.0 and -2.0 mm day^{-1}. In (a), positive values show BLs and negative values show compensated layers. Panels (c)-(f) use the same color scale as (b). Units are meters. JRE

Seasonal climatologies (e.g., Figure S3) demonstrate that the tropical barrier layers are present throughout the year, while the midlatitude barrier layers are mostly limited to the winter hemisphere. The ESMs capture this seasonal variation, and accord-

ingly have biases in the tropics throughout the year and biases in midlatitudes mostly limited to the winter hemisphere.

The BLT biases can be thought of as the superposition of biases in MLD~~the mixed layer depth~~[JRE] (i.e., ~~the~~ [JRE]top of the BL) and TTD~~the top of the thermocline depth~~[JRE] (i.e, ~~the~~ [JRE]bottom of the BL). For TTD (Figure S4), E3SM-C and GFDL-ECDA-v3.1 have negative biases (TTD too shallow) [JRE]in the tropics, and positive biases (TTD too deep) [JRE]in midlatitudes, similar to the BLT biases. The pattern of TTD biases for CESM2 is more complicated but again bears a strong resemblance to the BLT bias in Figure 1d. For MLD (Figure S5), E3SM-C and GFDL-ECDA-v3.1 generally have biases that are the opposite sense to TTD in midlatitudes (and therefore combine to give larger BLT biases), but the same sense in the tropics (and therefore partially cancel to give smaller BLT biases). For CESM2, MLD biases and TTD biases are largely of the same sign in both midlatitudes and tropics, leading to partial cancellation in BLT biases.

3.2 Effects on mixed layer entrainment

Much of the early interest in BLs stemmed from their ability to reduce entrainment of cold water from the thermocline into the mixed layer. We examine model representation of this process by looking at the mixed layer (i.e., from the ocean surface to MLD) heat budgets of E3SM-C and E3SM-O. [JRE]Figure 2 shows the long-term annual mean potential temperature tendency in the mixed layer due to vertical mixing from the two runs, and their difference. As expected, the tendencies are negative at the vast majority of grid points where cold thermocline water is mixed into the mixed layer, though a few grid points have positive values likely due to persistent temperature inversions. 60°S-60°N mean values are -0.021 °C day^{-1} in E3SM-C and -0.016 °C day^{-1} in E3SM-O. Tropical regions with BLs have relatively low rates of entrainment cooling, but are not the only such regions (especially in E3SM-O). Spatial correlations between BLT and entrainment cooling are 0.25 for E3SM-C and 0.18 for E3SM-O. These modest correlations, and the even lower values in midlatitudes, suggest that the presence, or otherwise, of a BL is not the dominant control on the spatial pattern of entrainment cooling.

The differences in entrainment cooling between E3SM-C and E3SM-O (Figure 2c; mean absolute difference 0.008 °C day^{-1}) bear some resemblance to the differences in BLT between the two runs (contours in Figure 2c). In particular, tropical regions with

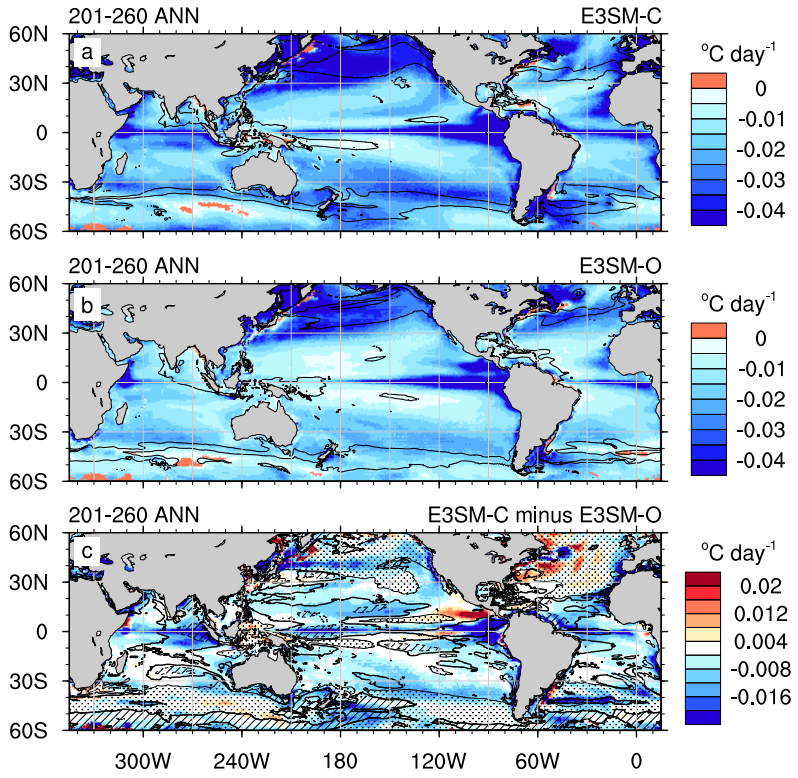

Figure 2. Long-term annual mean contribution of vertical mixing to the temperature tendency of the mixed layer: (a) E3SM-C; (b) E3SM-O; (c) difference (E3SM-C minus E3SM-O). Contour lines overlaid in (a) and (b) are long-term annual mean BLT at 10, 20 and 50 m. Contour lines overlaid in (c) are long-term annual mean BLT difference (coupled minus ocean-sea ice) at -5 m (thin dashed), 0 (thick solid), and 5 m (thin solid). In addition, areas with BLT difference $<$ -5 m are hatched and areas with BLT difference $>$ 5 m are stippled.

a negative BLT difference (i.e., thinner in the coupled run) have negative entrainment cooling differences (more entrainment in the coupled run). Likewise, some tropical regions with positive BLT difference have positive entrainment differences. The South Pacific convergence zone (SPCZ) is a notable exception to this — it has positive BLT difference but close to zero difference in entrainment cooling. In several regions, especially in midlatitudes, there is some difference in the entrainment cooling between the runs that cannot be explained by BLT differences — including, of course, in regions where BLs do not generally occur. Nonetheless, the correlation coefficient between tropical (30°S to 30°N) BLT difference and entrainment cooling difference is 0.56 (only considering grid

points where either model run has absolute value of annual mean BLT > 5.0 m). This result shows that BLs play an important role in the heat budget of the upper tropical oceans, and model deficiencies in simulating barrier layers can result in erroneous simulation of heat exchange across the thermocline.

3.3 Attribution of BLT biases

Next, we attempt to attribute BLT biases in E3SM-C to different components. To do this we focus on E3SM-O, which has active ocean and sea ice model components, forced by CORE2 atmospheric and river runoff reanalysis (Large & Yeager, 2009). Under the assumption that the CORE2 forcing does not include major observational errors, it follows that the biases in E3SM-O (Figure 1e) are primarily due to the ocean and sea ice models. The difference between E3SM-C and E3SM-O should then show the biases introduced primarily by the other model components (particularly the atmosphere model) and by coupling effects. The assumption about CORE2 is not unreasonable, because CORE2~~it~~[JRE] is derived from various observations and reanalysis. However, the assumption~~it~~[JRE] is not totally valid, potentially causing ~~and therefore erroneously attributes~~[JRE] biases introduced by CORE2 to be misattributed to[JRE] E3SM's ocean model, and complicating~~complicates~~[JRE] interpretation of biases caused by other model components.

Comparison of Figure 1c and 1e shows that much of the midlatitude and part of the tropical BLT biases are common to both runs, and thus suggests that these biases are caused by the ocean and sea ice models. However, there are clear differences in some regions, shown more clearly in Figure 1f. We note in particular differences in both the tropics (the Maritime Continent and West Pacific warm pool, the Bay of Bengal, the SPCZ, the Caribbean Sea and the mouth of the Amazon) and the midlatitudes (particularly south of 50°S, where E3SM-O has significantly larger positive biases than E3SM-C). It is likely that atmosphere (through fluxes of freshwater, momentum and heat) and land (through runoff) model biases, or complex interactions between model components, have an effect on BLT biases in these regions.

Salinity restoring in E3SM-O slightly complicates the above comparison between E3SM-C and E3SM-O. However, comparison of salinity restoring magnitude with surface freshwater fluxes (Figure S6) suggests that salinity restoring is the dominant freshwater forcing only in coastal regions and the North Atlantic and that it is relatively unim-

portant in the tropics. Therefore, of the tropical regions noted in the previous paragraph, salinity restoring likely has the largest effect on BLT differences around the mouth of the Amazon, in the Bay of Bengal, and to a lesser extent in the Caribbean Sea. However, the fact that E3SM-C has around 30% less Amazon runoff than E3SM-O (Figure S7) suggests that salinity restoring is not the only cause of these differences, and that atmosphere and land model biases make a non-trivial contribution. Some parts of the Southern Ocean have moderately strong salinity restoring too. However, because there is no clear spatial correspondence between salinity restoring and BLT differences (as was the case for, e.g., the Amazon) it is unclear if salinity restoring affects E3SM-O BLs here.

We expect the atmospheric model to contribute to BLT biases via freshwater input (precipitation minus evaporation, denoted (P-E)) and wind stress magnitude (τ). (These quantities are related: wind speed strongly affects both τ and evaporation. Both are analyzed as they affect upper ocean stratification in different ways and their relative importance may differ regionally.) (P-E) biases are shown for the three coupled model runs in Figure 1 (black contour lines), with the largest biases in the tropics. In all models, positive biases of BLT and (P-E) coincide in the Maritime Continent region, and negative biases of BLT and (P-E) coincide in the equatorial west Pacific. However, there are regions with large (P-E) biases and only small BLT biases (e.g., the tropical Atlantic in E3SM-C), and in the South Pacific Convergence Zone we even see negative BLT bias coincident with positive (P-E) bias — opposite to what is expected. Given that E3SM-O also shows a negative BLT bias it is likely that ocean dynamics are the dominant cause of the BLT bias in the SPCZ. In fact the magnitude of bias is larger (Figure 1f) in E3SM-O than E3SM-C, suggesting that the (P-E) bias acts in the expected direction.

Figure 3a shows the relationship between (P-E) and BLT biases more clearly: while there is noise in the relationship, tropical annual mean (P-E) biases are positively correlated with annual mean BLT biases. Results for CESM2 (Figure S8a) and GFDL-ECDA-v3.1 (Figure S9a) are similar, with surprisingly consistent regression slopes of around 1 m/(mm day^{-1}). The relationship between tropical wind stress (τ) biases and BLT (Figure 3d) is not as clear: neither correlation coefficients nor visual inspection suggest a significant relationship. The same holds for CESM2 (Figure S8d), though there is a suggestion of some correlation between τ and BLT biases for GFDL-ECDA-v3.1 (Figure S9d). Note that analyses in Figures 3, S8 and S9 are limited to grid points with long-term annual mean observed BLT greater than 5 m.

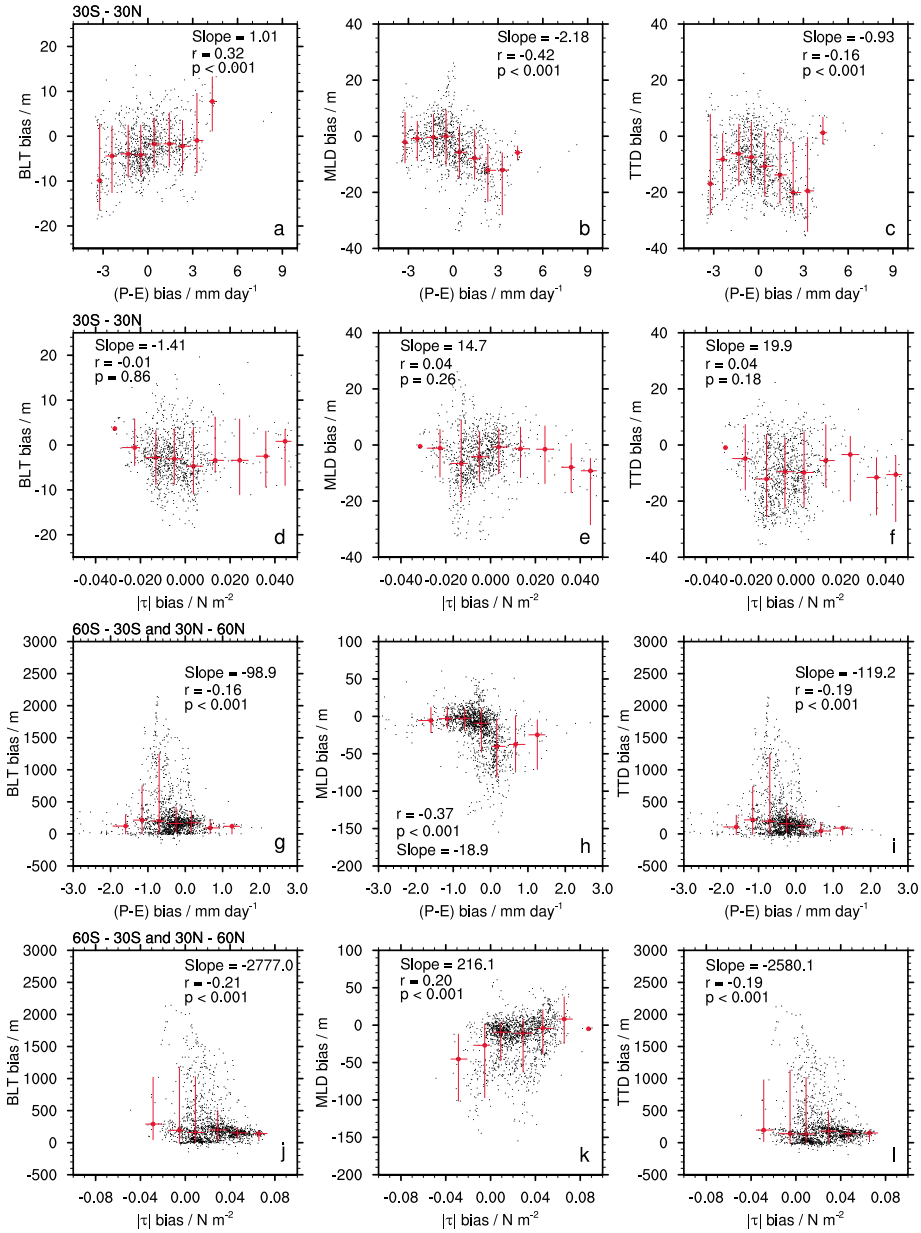

Figure 3. Scatter plots of long term annual mean biases in E3SM-C: BLT (left), MLD (middle) and TTD (right) bias versus (P-E) (first and third rows) and τ (second and fourth rows) bias. Panels a-f are for the tropics and g-l are for mid-latitudes. Black dots show individual grid point values, while red circles represent median values of bin quantities and lines represent 10th and 90th percentiles. Regression statistics shown for each plot are based on the individual grid points (black dots). This analysis includes only grid points that have absolute value of observed long term annual mean barrier layer thickness of 5 m or greater.

The greatest influence of atmosphere model biases on tropical BLT is mediated by the negative relationship between MLD and (P-E) biases (Figure 3b) . This is partially canceled by a weak negative relationship between (P-E) and TTD biases (Figure 3c), resulting in the positive relationship seen in Figure 3a. As with BLT, the relationships between MLD/TTD and τ biases (Figure 3 e and f) are weaker than with (P-E). Between 30° and 60° latitude (in both hemispheres), BLT biases are dominated by large positive TTD biases, which occur with negative (P-E) biases (Figure 3 g and i). As in the tropics, there is a moderately strong negative relationship between MLD and (P-E) biases (Figure 3h). In addition there is a weak (but significant) positive relationship between MLD and τ biases (Figure 3k), though this has limited influence on the BLT–τ relationship because of the dominance of TTD biases in midlatitudes. The results shown in Figure 3 are similar to results from CESM2 and GFDL-ECDA-v3.1 (Figures S8 and S9) ~~so the reasoning in this paragraph largely applies to them too~~[JRE].

4 Summary and discussion

We have compared mean BLT from E3SMv1 (i.e., E3SM-C and E3SM-O) with an observation-based climatology. In general, E3SMv1 captures the observed spatial distribution and seasonality of BLs. This is an encouraging result for model fidelity, particularly when considering the relatively coarse model vertical resolution in comparison to tropical BLTs. However, model BLT biases do exist: E3SMv1 has semi-permanent tropical BLs too thin, and seasonally occurring midlatitude BLs too thick and extending too far equatorward. CESM2 and the GFDL-ECDA-v3.1 reanalysis have broadly similar biases. Notably, though, GFDL-ECDA-v3.1 has smaller biases in the tropical Pacific, and the smallest globally averaged mean BLT bias. Data assimilation used in GFDL-ECDA-v3.1 likely contributes to its relatively good performance, though we cannot say this conclusively without assessment of a free-running variant of the GFDL model. For E3SMv1, large [JRE]midlatitude BLT biases have contributions from both MLD and TTD biases, while in many tropical regions MLD and TTD biases are of the same sense and therefore partially cancel in the BLT bias. Notably, this cancellation does not occur for E3SMv1 in the equatorial Pacific, resulting in relatively large BLT biases.

Through analysis of the E3SMv1 ocean model mixed layer temperature tendency, we have shown that the insulation effect of BLs is more apparent in the tropics than at higher latitudes. In the tropics, differences (between coupled and ocean-sea ice runs) in

entrainment cooling correspond to differences in BLT. This confirms that biases in BLT are able to affect transfer of heat across the thermocline. Whether this effect is important enough to affect simulations of long-term surface temperature change is worth investigation. Indeed, we suggest that BLT should be routinely analyzed in models contributing to the upcoming Coupled Model Intercomparison Project phase six (CMIP6) — both in model development and in data released for the various experiments. The present work marks a starting point for understanding how BLs can mediate links between biases in different model components — especially atmosphere and ocean.

Comparison between coupled and ocean-sea ice runs of E3SMv1 suggests that part of the tropical BLT bias in the coupled run comes from atmosphere, land or river-routing components or coupling between components. Comparison of coupled model BLT, MLD and TTD biases with (P-E) and wind stress biases shows that the dominant contribution in the tropics comes from (P-E) effects on MLD. Despite significant relationships, however, the atmospheric model contribution is only a fraction of the total BLT bias (as suggested by the noise in Figure 3). In midlatitudes, both (P-E) and wind stress biases affect MLD biases, but similarity of midlatitude BLT biases between E3SM-C and E3SM-O suggests that systematic ocean model biases dominate poleward of 30° (e.g., large positive TTD biases related to sub-surface temperature biases.~~ The ocean model biases manifest as large positive TTD biases caused by sub-surface temperature biases and possibly related to overly strong temperature inversions.~~[JRE]

The above analysis of BLT, MLD and TTD links to (P-E) and wind stress assumes that the observed correlations occur due to local effects, e.g., erroneously strong winds causing an in situ positive MLD bias. However, it is also possible that non-local effects may contribute to the relationships seen here. For example, in the Southern Ocean where BLs are caused by complex interactions of different water masses (Pan et al., 2018), wind stress biases over the entire region may affect BLs at a particular location, through model misrepresentation of ocean circulation. Nonetheless, we feel that the correlations presented here are indicative of local linkages of model bias in many regions, particularly in the tropics where observational evidence of relevant processes exists (e.g., Lukas & Lindstrom, 1991; Anderson et al., 1996).

We end by noting that most of the model biases we have investigated relate to two or more model components, and so reducing the biases is more difficult than address-

ing issues in individually forced model configurations. We advocate several areas of model sensitivity tests that could aid in the process: ocean model sensitivity to precipitation variation (to confirm our attribution of BLT biases and assess resulting SST effects); atmosphere model precipitation sensitivity to SST variation (to assess whether a feedback can exist between BLT, SST and precipitation); and ocean model sensitivity to river discharge and salinity restoring (to test the assumption that E3SM-O biases are due only to the ocean model, rather than these quite uncertain aspects of the forcing).

Acknowledgments

This research was supported as part of the Energy Exascale Earth System Model (E3SM) project, funded by the U.S. Department of Energy (DOE), Office of Science, Office of Biological and Environmental Research. JRE, XZ and MAB were supported by DOE under grant DE-SC0016533. Work at Lawrence Livermore National Laboratory was performed under the auspices of DOE under Contract DE-AC52-07NA27344. This work was supported by DOE through the Los Alamos National Laboratory, which is operated by Triad National Security, LLC, for the DOE National Nuclear Security Administration under Contract No. 89233218CNA000001. Approved for unlimited release - LA-UR-19-20158. The E3SMv1 simulations were run and analyzed on Edison, a resource of the National Energy Research Scientific Computing Center, a DOE Office of Science User Facility supported under Contract No. DE-AC02-05CH11231; and on Anvil, a high-performance computing cluster provided by the Office of Biological and Environmental Research Earth System Modeling program and operated by the Laboratory Computing Resource Center at Argonne National Laboratory. We would like to acknowledge high-performance computing support for CESM2 simulations and analysis from Cheyenne (doi:10.5065/D6RX99HX) provided by NCAR's Computational and Information Systems Laboratory, sponsored by the National Science Foundation. Figures were created using NCAR Command Language (NCL, 2019). Computer code and data used in this analysis are available from `https://osf.io/v9fbk/?view_only=fad2fae3c8824c4c86b945ef62f8b254`.

References

Adler, R. F., Huffman, G. J., Chang, A., Ferraro, R., Xie, P.-P., Janowiak, J., ... Nelkin, E. (2003). The Version-2 Global Precipitation Climatology Project (GPCP) Monthly Precipitation Analysis (1979–Present). *J. Hydrometeor.*,

4(6), 1147-1167. doi: 10.1175/1525-7541(2003)004⟨1147:TVGPCP⟩2.0.CO;2

Adler, R. F., Huffman, G. J., Chang, A., Ferraro, R., Xie, P.-P., Janowiak, J., ... Nelkin, E. (2017). *GPCP Version 2.3 Combined Precipitation Data Set* [Dataset]. National Oceanic and Atmospheric Administration (NOAA) Earth System Research Laboratory (ESRL) Physical Sciences Division. Retrieved 04 Oct 2017, from `https://www.esrl.noaa.gov/psd/data/gridded/data.gpcp.html`

Anderson, S. P., Weller, R. A., & Lukas, R. B. (1996). Surface Buoyancy Forcing and the Mixed Layer of the Western Pacific Warm Pool: Observations and 1D Model Results. *J. Climate*, *9*(12), 3056-3085. doi: 10.1175/1520-0442(1996)009⟨3056:SBFATM⟩2.0.CO;2

Balaguru, K., Chang, P., Saravanan, R., & Jang, C. J. (2012). The barrier layer of the Atlantic warmpool: Formation mechanism and influence on the mean climate. *Tellus A: Dynamic Meteorology and Oceanography*, *64*(1), 18162. doi: 10.3402/tellusa.v64i0.18162

Balaguru, K., Chang, P., Saravanan, R., Leung, L. R., Xu, Z., Li, M., & Hsieh, J.-S. (2012). Ocean barrier layers' effect on tropical cyclone intensification. *PNAS*, *109*(36), 14343-14347. doi: 10.1073/pnas.1201364109

Bosc, C., Delcroix, T., & Maes, C. (2009). Barrier layer variability in the western Pacific warm pool from 2000 to 2007. *Journal of Geophysical Research: Oceans*, *114*(C6). doi: 10.1029/2008JC005187

Breugem, W.-P., Chang, P., Jang, C. J., Mignot, J., & Hazeleger, W. (2008). Barrier layers and tropical Atlantic SST biases in coupled GCMs. *Tellus A*, *60*(5), 885-897. doi: 10.1111/j.1600-0870.2008.00343.x

Chang, Y.-S., Zhang, S., Rosati, A., Delworth, T. L., & Stern, W. F. (2013). An assessment of oceanic variability for 1960–2010 from the GFDL ensemble coupled data assimilation. *Clim Dyn*, *40*(3-4), 775-803. doi: 10.1007/s00382-012-1412-2

Cronin, M. F., & McPhaden, M. J. (2002). Barrier layer formation during westerly wind bursts. *Journal of Geophysical Research: Oceans*, *107*(C12), SRF 21-1. doi: 10.1029/2001JC001171

de Boyer Montégut, C., Durand, F., Bourdallé-Badie, R., & Blanke, B. (2014). Role of fronts in the formation of Arabian Sea barrier layers during summer

monsoon. *Ocean Dynamics*, *64*(6), 809-822. doi: 10.1007/s10236-014-0716-7

de Boyer Montégut, C., Madec, G., Fischer, A. S., Lazar, A., & Iudicone, D. (2004). Mixed layer depth over the global ocean: An examination of profile data and a profile-based climatology. *Journal of Geophysical Research: Oceans*, *109*(C12). doi: 10.1029/2004JC002378

de Boyer Montégut, C., Mignot, J., Lazar, A., & Cravatte, S. (2007). Control of salinity on the mixed layer depth in the world ocean: 1. General description. *J. Geophys. Res.*, *112*(C6), C06011. doi: 10.1029/2006JC003953

de Boyer Montégut, C., Mignot, J., Lazar, A., & Cravatte, S. (2009). *IFREMER/LOS Mixed Layer Depth Climatology* [Dataset]. French Research Institute for Exploration of the Sea (IFREMER) Spatial Oceanography Laboratory (LOS). Retrieved 08 Jun 2018, from `http://www.ifremer.fr/cerweb/deboyer/mld/gridded_data.php`

Drushka, K., Sprintall, J., & Gille, S. T. (2014). Subseasonal variations in salinity and barrier-layer thickness in the eastern equatorial Indian Ocean. *Journal of Geophysical Research: Oceans*, *119*(2), 805-823. doi: 10.1002/2013JC009422

Duffy, P. B., & Caldeira, K. (1997). Sensitivity of simulated salinity in a three-dimensional ocean model to upper ocean transport of salt from sea-ice formation. *Geophysical Research Letters*, *24*(11), 1323-1326. doi: 10.1029/97GL01294

E3SM Project. (2018). Energy Exascale Earth System Model (E3SM) [Computer software]. `https://dx.doi.org/10.11578/E3SM/dc.20180418.36`. doi: 10.11578/E3SM/dc.20180418.36

Foltz, G. R., Grodsky, S. A., Carton, J. A., & McPhaden, M. J. (2004). Seasonal salt budget of the northwestern tropical Atlantic Ocean along 38°W. *Journal of Geophysical Research: Oceans*, *109*(C3). doi: 10.1029/2003JC002111

Foltz, G. R., & McPhaden, M. J. (2009). Impact of Barrier Layer Thickness on SST in the Central Tropical North Atlantic. *J. Climate*, *22*(2), 285-299. doi: 10.1175/2008JCLI2308.1

Geophysical Fluid Dynamics Laboratory. (2013). *Geophysical Fluid Dynamics Laboratory Ensemble Coupled Data Assimilation, version 3.1 (GFDL-ECDA-v3.1)* [Dataset]. Retrieved 11 Jun 2018, from `ftp://ftp.gfdl.noaa.gov/perm/wga/ECDA_v3.1/`

Godfrey, & Lindstrom. (1989). The heat budget of the equatorial western Pacific surface mixed layer. *Journal of Geophysical Research: Oceans*, *94*(C6), 8007-8017. doi: 10.1029/JC094iC06p08007

Golaz, J.-C., Caldwell, P. M., Roekel, L. P. V., Petersen, M. R., Tang, Q., Wolfe, J. D., ... Zhu, Q. (2019). The DOE E3SM coupled model version 1: Overview and evaluation at standard resolution. *Journal of Advances in Modeling Earth Systems*, *0*(ja). doi: 10.1029/2018MS001603

Holte, J., Talley, L. D., Gilson, J., & Roemmich, D. (2017). An Argo mixed layer climatology and database. *Geophysical Research Letters*, *44*(11), 5618-5626. doi: 10.1002/2017GL073426

Hurrell, J. W., Holland, M. M., Gent, P. R., Ghan, S., Kay, J. E., Kushner, P. J., ... Marshall, S. (2013). The Community Earth System Model: A Framework for Collaborative Research. *Bull. Amer. Meteor. Soc.*, *94*(9), 1339-1360. doi: 10.1175/BAMS-D-12-00121.1

Kara, A. B., Rochford Peter A., & Hurlburt Harley E. (2000). Mixed layer depth variability and barrier layer formation over the North Pacific Ocean. *Journal of Geophysical Research: Oceans*, *105*(C7), 16783-16801. doi: 10.1029/2000JC900071

Large, W. G., & Yeager, S. G. (2009). The global climatology of an interannually varying air-sea flux data set. *Climate Dynamics; Heidelberg*, *33*(2-3), 341-364. doi: http://dx.doi.org.ezproxy4.library.arizona.edu/10.1007/s00382-008-0441-3

Lukas, R., & Lindstrom, E. (1991). The mixed layer of the western equatorial Pacific Ocean. *J. Geophys. Res.*, *96*(S01), 3343-3357. doi: 10.1029/90JC01951

Maes, C., Picaut, J., & Belamari, S. (2002). Salinity barrier layer and onset of El Niño in a Pacific coupled model. *Geophys. Res. Lett.*, *29*(24), 2206. doi: 10.1029/2002GL016029

Maes, C., Picaut, J., & Belamari, S. (2005). Importance of the Salinity Barrier Layer for the Buildup of El Niño. *J. Climate*, *18*(1), 104-118. doi: 10.1175/JCLI-3214.1

McDougall, T. J., & Barker, P. M. (2011). Getting started with TEOS-10 and the Gibbs Seawater (GSW) Oceanographic Toolbox [Computer software manual]. Scientific Committee on Oceanic Research/International Association for the

Physical Sciences of the Oceans, Working Group 127.

Mignot, J., de Boyer Montégut, C., Lazar, A., & Cravatte, S. (2007). Control of salinity on the mixed layer depth in the world ocean: 2. Tropical areas - Mignot - 2007 - Journal of Geophysical Research: Oceans - Wiley Online Library. *Journal of Geophysical Research - Oceans*, *112*(C10). doi: 10.1029/2006JC003954

Mignot, J., de Boyer Montégut, C., & Tomczak, M. (2009). On the porosity of barrier layers. *Ocean Sci.*, *5*(3), 379-387. doi: 10.5194/os-5-379-2009

Mignot, J., Lazar, A., & Lacarra, M. (2012). On the formation of barrier layers and associated vertical temperature inversions: A focus on the northwestern tropical Atlantic. *Journal of Geophysical Research: Oceans*, *117*(C2). doi: 10.1029/2011JC007435

National Center for Atmospheric Research (NCAR). (2018). Community Earth System Model version 2 (CESM2) [Computer software]. `http://www.cesm.ucar.edu/models/cesm2/`.

NCL. (2019). NCAR Command Language (version 6.3.0) [Computer software]. Boulder, Colorado: UCAR/NCAR/CISL/TDD. doi: http://dx.doi.org/10.5065/D6WD3XH5

Nguyen, A. T., Menemenlis, D., & Kwok, R. (2009). Improved modeling of the Arctic halocline with a subgrid-scale brine rejection parameterization. *Journal of Geophysical Research: Oceans*, *114*(C11). doi: 10.1029/2008JC005121

Pailler, K., Bourlès, B., & Gouriou, Y. (1999). The barrier layer in the western tropical Atlantic Ocean. *Geophysical Research Letters*, *26*(14), 2069-2072. doi: 10.1029/1999GL900492

Pan, L., Zhong, Y., Liu, H., Zhou, L., Zhang, Z., & Zhou, M. (2018). Seasonal Variation of Barrier Layer in the Southern Ocean. *Journal of Geophysical Research: Oceans*, *0*(0). doi: 10.1002/2017JC013382

Petersen, M. R., Asay-Davis, X. S., Berres, A. S., Chen, Q., Feige, N., Hoffman, M. J., ... Woodring, J. L. (2019). An evaluation of the ocean and sea ice climate of E3SM using MPAS and interannual CORE-II forcing. *Journal of Advances in Modeling Earth Systems*, *0*(ja). doi: 10.1029/2018MS001373

Sato, K., Suga, T., & Hanawa, K. (2006). Barrier layers in the subtropical gyres of the world's oceans. *Geophysical Research Letters*, *33*(8). doi: 10.1029/

2005GL025631

Shenoi, S. S. C., Shankar, D., & Shetye, S. R. (2002). Differences in heat budgets of the near-surface Arabian Sea and Bay of Bengal: Implications for the summer monsoon. *Journal of Geophysical Research: Oceans*, *107*(C6), 5-1-5-14. doi: 10.1029/2000JC000679

Sprintall, J., & Tomczak, M. (1992). Evidence of the barrier layer in the surface layer of the tropics. *Journal of Geophysical Research: Oceans*, *97*(C5), 7305-7316. doi: 10.1029/92JC00407

Steele, M., & Boyd, T. (1998). Retreat of the cold halocline layer in the Arctic Ocean. *Journal of Geophysical Research: Oceans*, *103*(C5), 10419-10435. doi: 10.1029/98JC00580

TEOS-10 Project. (2017). Thermodynamic Equation Of State 2010 (TEOS-10) Gibbs-SeaWater (GSW) Oceanographic Toolbox, version 3.05-6 for Fortran [Computer software]. Retrieved 23 Mar 2018, from `http://www.teos-10.org/software.htm`

Vialard, J., & Delecluse, P. (1998). An OGCM Study for the TOGA Decade. Part II: Barrier-Layer Formation and Variability. *J. Phys. Oceanogr.*, *28*(6), 1089-1106. doi: 10.1175/1520-0485(1998)028⟨1089:AOSFTT⟩2.0.CO;2

Yeager, S. G., & Large, W. G. (2008). *Core.2 global air-sea flux dataset* [Dataset]. Research Data Archive at the National Center for Atmospheric Research, Computational and Information Systems Laboratory, Boulder, Colo. (Updated irregularly.). Retrieved 11 Jun 2018, from `https://doi.org/10.5065/D6WH2N0S`

You, Y. (1998). Rain-formed barrier layer of the western equatorial Pacific warm pool: A case study. *Journal of Geophysical Research: Oceans*, *103*(C3), 5361-5378. doi: 10.1029/97JC03421

Yu, L., Jin, X., & Weller, R. A. (2006). *Objectively Analyzed Air-Sea Fluxes (OAFlux) For Global Oceans* [Dataset]. Woods Hole Oceanographic Institution, Physical Oceanography Department. Retrieved 05 May 2018, from `ftp://ftp.whoi.edu/pub/science/oaflux/data_v3/monthly/evaporation/`

Yu, L., & Weller, R. A. (2007). Objectively Analyzed Air–Sea Heat Fluxes for the Global Ice-Free Oceans (1981–2005). *Bull. Amer. Meteor. Soc.*, *88*(4), 527-540.

593 doi: 10.1175/BAMS-88-4-527

594 Zhi, H., Zhang, R.-H., Zheng, F., Lin, P., Wang, L., & Yu, P. (2016). Assessment of
595 interannual sea surface salinity variability and its effects on the barrier layer in
596 the equatorial Pacific using BNU-ESM. *Adv. Atmos. Sci.*, *33*(3), 339-351. doi:
597 10.1007/s00376-015-5163-y

598 Zhu, J., Huang, B., Zhang, R.-H., Hu, Z.-Z., Kumar, A., Balmaseda, M. A., ... Iii,
599 J. L. K. (2014). Salinity anomaly as a trigger for ENSO events. *Scientific*
600 *Reports*, *4*, 6821. doi: 10.1038/srep06821